Traffic 2009; **10:** 1579–1584

doi:10.1111/j.1600-0854.2009.00980.x

Toolbox

Live Cell Multicolor Imaging of Lipid Droplets with a New Dye, LD540

Johanna Spandl[1], Daniel J. White[1], Jan Peychl[1] and Christoph Thiele[1,2,*]

[1]Max Planck Institute of Molecular Cell Biology and Genetics, Pfotenhauerstr. 108, 01307 Dresden, Germany
[2]LIMES Life and Medical Sciences Institute, University of Bonn, Carl-Troll-Strasse 31, 53115 Bonn, Germany
**Corresponding author: Christoph Thiele, cthiele@uni-bonn.de*

A lipophilic dye based on the Bodipy fluorophore, LD540, was developed for microscopic imaging of lipid droplets. In contrast to previous lipid droplet dyes, it can spectrally be resolved from both green and red fluorophores allowing multicolor imaging in both fixed and living cells. Its improved specificity, brightness and photostability support live cell imaging, which was used to demonstrate by two-color imaging lipid droplet motility along microtubules.

Key words: lipid droplets, live cell microscopy, 3T3-L1 adipocytes, HuH7 hepatoma cells

Received 6 May 2009, revised and accepted for publication 20 August 2009, uncorrected manuscript published online 2 September 2009, published online 17 September 2009

Lipid droplets (LDs) are the cellular organelles that store triglyceride and other neutral lipids. They consist of a core of neutral lipids, surrounded by a monolayer of phospholipids with attached or embedded proteins. LDs are dynamic organelles, which are formed and degraded, move inside cells and also may undergo fusion. To study their morphological and dynamic relation to other cellular organelles, multicolor fluorescence imaging of fixed specimens or living cells is an essential tool. Because LDs form functional and morphological subpopulations (1), no single marker protein exists that would stain the entire LD pool of a cell. Therefore, the only reliable way to visualize all droplets in a given cell is by staining the LD core with lipophilic dyes. So far, mainly two dyes, Nile Red and Bodipy 493/503, have been used for this purpose (2,3). Nile Red displays strong solvatochromism and broad excitation and emission bands, being visible using filter sets for both green and red dyes (see Supporting Information Figure S1A for spectra of the LD dyes). Nonetheless, Nile Red can be imaged together with enhanced green fluorescent protein (EGFP) for applications that do not require complete separation of channels (4), but addition of other yellow, orange or far-red dyes is not possible. Bodipy 493/503 can be spectrally separated from many red fluorescent dyes and proteins, but not from the popular fluorescent proteins, enhanced cyan, green and yellow fluorescent protein (ECFP, EGFP, EYFP), or fluorophores with similar properties, precluding multicolor imaging in living cells. A recent addition is two red fluorescent LD dyes, LipidTox red and LipidTox far red, that can be spectrally separated from green fluorophores and have occasionally been used for LD staining (5). Judged on the pictures provided by the manufacturer (6), there seem to be considerable problems with background staining. There is no publication that describes the dyes' properties, and the manufacturer does not disclose their chemical identity and sells them currently for about 200-fold the price of Bodipy 493/503. To find a generally applicable solution to the problem of multicolor imaging of LDs, we looked for lipophilic dyes with spectral properties compatible with the most frequently used fluorescent proteins. Because the Bodipy fluorophore as such has several favorable properties, we searched the Bodipy literature for a lipophilic dye that should be (i) redshifted relative to Bodipy 493/503 to allow spectral separation from green fluorescent protein (GFP), (ii) lipophilic enough to partition into LDs, (iii) have a symmetric structure that can be built in a one-pot reaction from (iv) commercially available precursors to allow economic synthesis. We identified as a candidate 4,4-difluoro-2.3,5.6-bis-tetramethylene-4-bora-3a,4a-diaza-*s*-indacene (LD540, Figure 1A), compound 14 in the review by Loudet and Burgess (7), originally published as compound 7 h in the patent by Morgan and Boyer (8), with reported excitation and emission maxima of 535 and 560 nm, respectively.

Results and Discussion

We synthesized the compound from tetrahydropyrrole, acetylchloride and BF_3-etherate and stained various cell lines according to the commonly used protocols for Bodipy 493/503 or Nile Red (9). At the concentrations typically used for Bodipy 493/503, staining by LD540 was much brighter, leading to oversaturated images. Reducing the dye concentration resulted in a bright, robust and highly specific yellow-green staining of LDs in all cell lines (Figure 1B). Because the absorption coefficient and the quantum yield of LD540 are similar to that of Bodipy 493/503 (8), brighter staining and increased specificity indicate stronger accumulation of the dye in the LDs. We measured log *P* values of both dyes for partitioning in different

Traffic

A

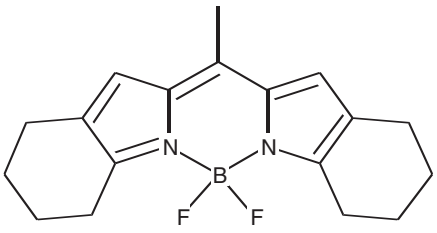

LD540

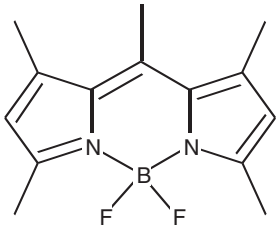

Bodipy 493/503

B

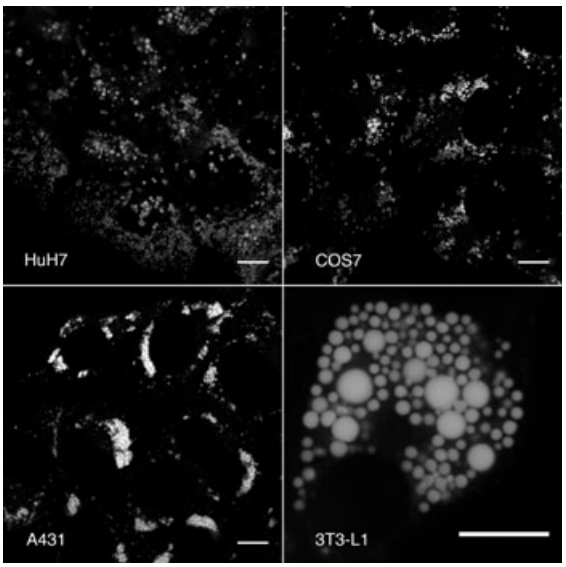

Figure 1: LD540 stains lipid droplets. A) Structures of LD540 and Bodipy 493/503. B) Formaldehyde-fixed cells as indicated were stained with a solution of 50 ng/mL LD540 in PBS for 10 min, washed with PBS and mounted in Mowiol/DABCO. Images were captured using a Zeiss LSM510 META confocal microscope with laser excitation at 543 nm and emission filtering using a LP560 filter. Unprocessed original tiff files are shown. Note the very small but well-defined LDs in HuH7 cells and the virtual lack of any background from nonspecific membrane staining. Bar: 10 μm.

solvent pairs and found a significantly higher lipophilicity of LD540 (Supporting Information Table S1). This allows use of LD540 in concentrations 10–20 times lower than Bodipy 493/503, reducing costs and background staining considerably. For use in multicolor imaging, we next studied its spectral properties under various conditions (Table S2). Solutions in different solvents were compared with a suspension of LD540-stained 3T3-L1 cells. Excitation maxima showed a small redshift with increasing lipophilicity of the solvent. Maxima obtained in stained cells (λ_{max} ex = 540 nm, λ_{max} em = 545 nm) were identical to those of the dye dissolved in sunflower oil, consistent with the presence of the dye in the intracellular LDs, which also consist mainly of triglycerides. For further analysis, we therefore used the spectra measured in oil because they optimally represent the dye's behavior in cells. Overlay with spectra of the various fluorescent proteins indicated the possibility of spectral resolution from the most popular fluorescent protein, EGFP (Figure S1B, for detailed spectral data in excel format also see Spectra Table S3). After optimization of microscope settings (see *Materials and Methods* for details), we could achieve bright, well-defined images in living cells [see Figure 2A for an example of co-staining the LD core with LD540 and the LD periphery with the LD protein ancient ubiquitous protein 1 (AUP1)]. These pictures were suitable for image analysis without the need of correction for excitation cross talk or emission bleed-through.

Further addition of blue and far-red fluorophores (for spectra see Figure S1C) allowed straightforward multicolor imaging. With appropriate laser lines and emission filters, separation of four colors is possible without the need of spectral imaging and mathematical linear unmixing of the four dyes. Using these settings, we could perform multicolor imaging in HuH7 hepatoma cells (Figure 2B) for nuclei (4',6-diamidino-2-phenylindole (DAPI), blue), a LD-associated protein (Rab18-EGFP, green), the LD core (LD540, red) and filamentous actin (Alexa647-phalloidin, magenta), which demonstrated the lack of colocalization of LDs with filamentous actin structures.

Apart from specificity and spectral properties, photostability is the third key feature of a neutral lipid dye, and it is of particular practical importance for imaging. It is limiting the usefulness of a dye for repeated high-resolution imaging needed for both time-resolved studies on living cells and modern high-resolution microscopy methods such as structured illumination or stimulated emission depletion microscopy (STED) microscopy (10). Because Bodipy 493/503 is rapidly bleached (9), previous attempts of live cell imaging of LDs have either used GFP-labeled LDs (11,12) or used Nile Red, the latter resulting in background problems particularly when smaller droplets were imaged in nonadipocytes (11). We found that the half-life ($t_{1/2}$) of LD540 under constant illumination in a fluorometer was about 15-fold larger than that of Bodipy 493/503, and threefold larger than that of Nile Red (Figure S2A). Under laser excitation at conditions practically used for imaging, LD540 was at least four times more stable than Bodipy 493/503 (Figure S2B). This stability prompted us to perform two-color live cell imaging of LDs, to visualize LD movement along microtubule tracks. So far, motility of LDs along microtubules had been demonstrated indirectly by

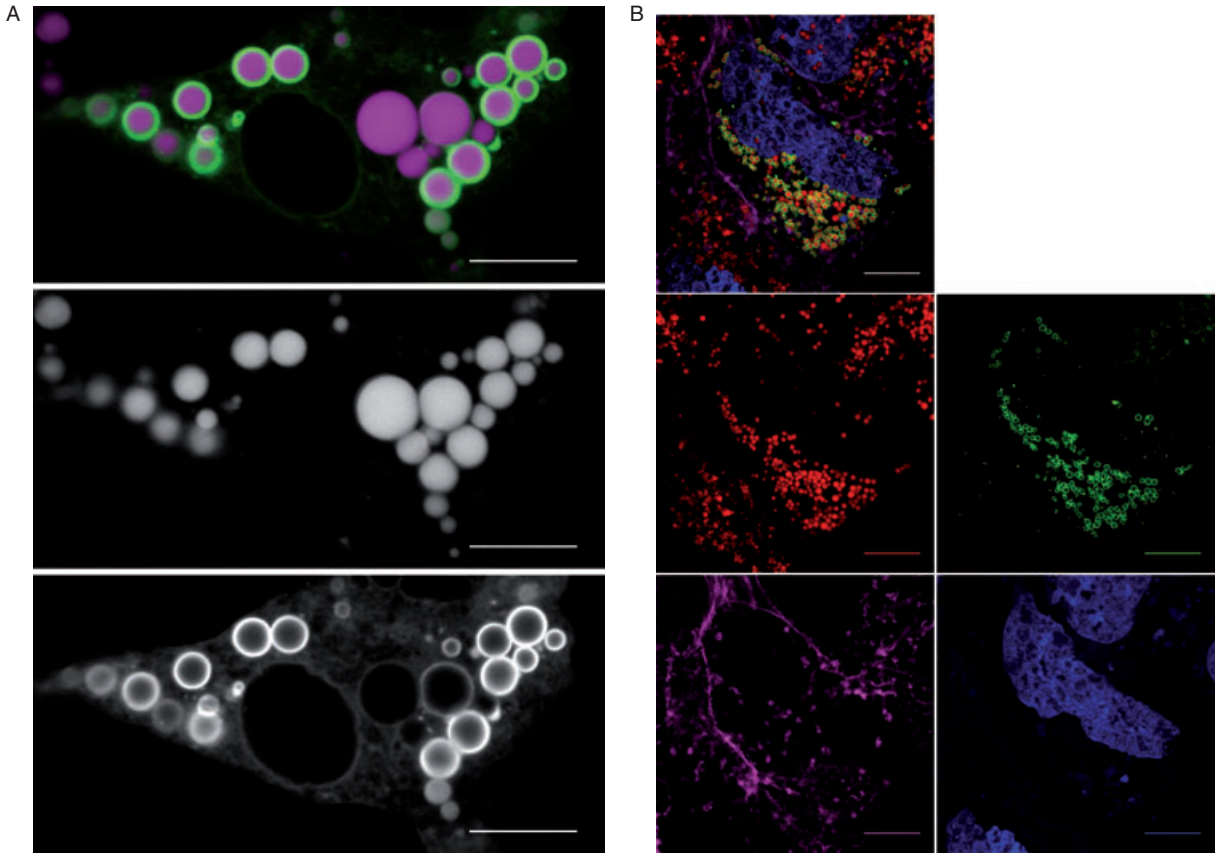

Figure 2: Live cell and multicolor imaging of lipid droplets. A) Live cell two-color imaging of 3T3-L1 cells transiently expressing AUP1-EGFP. Cells were stained with LD540 and imaged as described above. An overlay of green (AUP1-EGFP) and magenta (LDs) channels is shown together with the single unprocessed tiff files to demonstrate the complete separation of the two channels. B) Multicolor imaging of LDs in HuH7 hepatoma cells. HuH7 cells transiently expressing Rab18-EGFP (green) were fixed, permeabilized, and stained with Alexa647-phalloidin (magenta) for actin filaments, LD540 (red) for LDs and DAPI (blue) for DNA. Bar: 10 μm.

detailed genetic and biophysical analysis in drosophila embryos [see references (13,14) and references therein] or by analysis of LD motility after destruction of the microtubule network by nocodazole treatment (15). The association of LDs with microtubules has been shown in fixed cells (16,17). We transfected COS7 cells with pEGFP-α-tubulin (Clontech) and stained LDs with LD540. Movie S1 shows a series of 30 image frames taken at intervals of 4 seconds. Although a major fraction of LDs (magenta) oscillates around apparent microtubule attachment sites, some LDs show clear processive motility along the microtubule tracks (green). This is illustrated in Figure 3, which shows a series of eight sequential pictures of a small segment of the movie. A detailed study of kinetic parameters is beyond the scope of this study, but preliminary analysis of processive LD movements using MOTIONTRACKER software (Kalaimoscope) showed typical velocities of 0.2–0.4 μm/second with peak velocities of about 0.7 μm/second, consistent with the reported velocities of LDs in drosophila embryos (14) and in general with kinesin family motors (18).

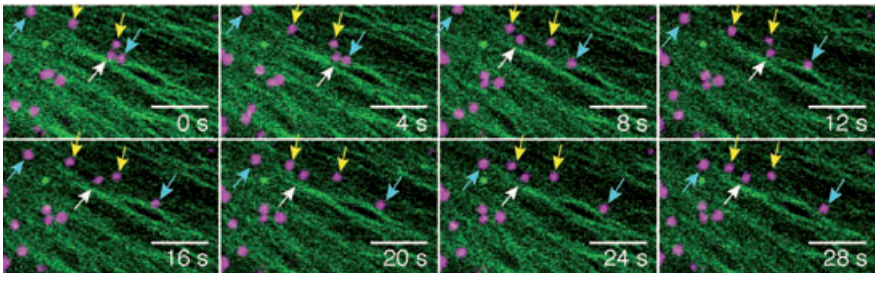

Figure 3: Closeup of the upper region of Movie S1, showing LDs (magenta) and microtubules (green). The nucleus with the microtubule organizing center (MTOC) is to the upper left side of this image detail. Some LDs (yellow arrows) are stationary, whereas others move either toward the nucleus (white arrow) or to the cell periphery (cyan arrows). Bar: 5 μm.

In conclusion, we present a new tool that allows multicolor imaging of LDs in live cells with high specificity, which will be helpful to explore the intracellular transport of neutral lipid and changes in the morphological organization of these fascinating organelles.

Materials and Methods

Synthesis of LD540

Synthesis was performed according to the general method given (8) with some minor modifications. Briefly, 1 g of tetrahydroindole was dissolved in 6 mL dry dichloromethane (DCM). Freshly distilled acetyl chloride (2 mL) was added dropwise. In an exothermic reaction, the solution turned dark red and was kept at 42°C for 1 h. The solvent was evaporated and the residue triturated with 2 × 10 mL hexane. The residue was dissolved in 100 mL DCM and 2.5 mL triethylamine and 2.45 mL BF_3-etherate were added. After stirring for 2 h, the solvent was evaporated and the residue subjected to silica gel chromatography using DCM/hexane 2/3 as a solvent.

Yield: 350 mg of 4,4-difluoro-2.3,5.6-bis-tetramethylene-4-bora-3a,4a-diaza-*s*-indacene (LD540, Figure 1A), purity > 95%. The product was stored in sealed ampoules in aliquots of 5 mg at −20°C.

Ultraviolet–Visible (UV–Vis) spectroscopy: $\lambda_{max} = 536$ nm, $\varepsilon = 89\,500$ mol^{-1} cm^{-1} (10 μM in ethanol) [Lit (8).: 535 nm, $\varepsilon = 85\,100$ $mol^{-1}cm^{-1}$]

Staining of cells with LD540

Fixed cells

For a stock solution, LD540 was dissolved in ethanol at 0.5 mg/mL, which was stored at −20°C. Cells were fixed with 4% paraformaldehyde, permeabilized with saponin and immunostained with antibodies as described previously (19). Cells were incubated with a solution of 0.05–0.1 μg/mL LD540 in PBS for 5–30 min, washed three times with PBS and once with water and mounted in Mowiol/Dabco as described (19). For some applications, it can be useful to avoid glycerol-containing mounting media such as Moviol, because they were reported to induce LD fusion (20). When antibody staining was not necessary, cells were only fixed without permeabilization and stained with LD540 as described above.

Living cells

Normal growth medium was exchanged for DMEM (without phenol red), 25 mM HEPES pH 7.4 (Gibco Nr. 21063) supplemented with 10% fetal calf serum (FCS) (live cell imaging medium, LCIM). Cells were stained with LD540 at 0.5 μg/mL in LCIM for 10 min followed by three washes with LCIM. The higher concentration of LD540 needed is probably due to the presence of large amounts of BSA in the FCS, which captures some of the dye.

Imaging LD540 on confocal laser scanning microscopes

Implementation of a new dye on existing microscopes usually is a compromise between considerations of costs, time, flexibility and image quality, as will become obvious in the comments on the settings given below. Changing laser lines and scan head filters, which might be necessary to get optimal images, causes major costs, loss of time, and may compromise other applications. Therefore, we developed microscope settings on two available Zeiss LSM510 instruments at the MPI-CBG light microscopy facility without any modifications of the instrument hardware. The settings developed should enable transfer to many other microscopes, also of other manufacturers. In order to assure broad applicability, we also did not make use of spectral detection, although a suitable Zeiss LSM510 META detector and an Olympus Fluoview FV1000 system were available. Even with suboptimal settings, good images were obtained, supported by the dye's exceptional brightness and stability.

Microscope settings for specific implementations

In the following, we use the Zeiss nomenclature for designation of beam splitters and filters:

The main dichroic beamsplitters are designated HFT XXX/YYY/... (HFT stands for HauptFarbTeiler) with XXX etc. being the wavelengths of the light deflected onto the specimen. Emitted fluorescent light is allowed to pass through the HFT to the detector.

The secondary dichroic beamsplitters are designated NFT XXX (NFT stands for NebenFarbTeiler). Light with shorter wavelength is deflected, light with longer wavelength passes the NFT.

An LP XXX (Long Pass) filter transmits emission light with wavelengths longer than the indicated threshold value XXX.

A BP XXX-YYY (Band Pass) transmits emission light within the indicated wavelength band.

One-color imaging

Any laser line between 488 and 543 nm can be used for excitation of LD540. When 488, 514 or 532 nm are used, the peak of emission can be collected with a suitable bandpass or longpass filter, depending on the necessity to reduce cellular background fluorescence. Excitation at 543 nm should be combined with a LP560 filter.

Two-color imaging at the Zeiss LSM510 META

EGFP: 458-nm line from a 40 mW Argon ion multi laser line at 14% laser power → HFT458/543 → sample → HFT458/543 → mirror → NFT515 → BP475-520 → detector 1

LD540: 543-nm laser from a 3 mW HeNe laser at 2% laser power → HFT458/543 → sample → HFT458/543 → mirror → NFT515 → Long pass filter LP560 → detector 2

Comment: These settings are optimized for a bright EGFP signal, combined with optimal separation of channels. The same beam splitters are used for both channels, which allows parallel imaging of the two channels for fast frame acquisition, that is, in living cells. Note that detector 1 effectively collects the EGFP emission between 475 and 515 nm because the NFT515 eliminates the light between 515 and 520 nm. This is important to exclude residual light emitted by LD540. LD540 is maximally excited at 543 nm with very low laser energy, resulting in extremely low photobleaching.

In general, these settings are close to optimal and result in excellent images. Potential for further improvement is in the use of a 532-nm laser line for excitation, which would allow to shift the emission filter for LD540 to slightly shorter wavelengths and collect even more light from the dye.

Three-color imaging at the Zeiss LSM510 META

EGFP: 458-nm line from a 40 mW Argon ion multi laser line at 14% laser power → HFT458/543 → sample → HFT458/543 → NFT635vis → NFT515 → BP475-520 → detector1

LD540: 543-nm laser from a 3 mW HeNe laser at 2% laser power → HFT458/543 → sample → HFT458/543 → NFT635vis → NFT515 → LP560 → detector2

Alexa647: 633-nm line from a 5 mW HeNe laser at 5% laser power → HFT514/633 → sample → HFT514/633 → NFT635vis → Plate → META detector 640–800 nm

Comment: This is based on the above two-color settings. An additional NFT635vis secondary dichroic mirror splits the beam to separate the

long wavelength emission. Because the 633-nm laser requires a different primary dichroic mirror, the third channel needs to be scanned separately, which precludes high frame rates. For the detection, we use the META detector, but only to substitute for a 640-nm long pass filter, which is lacking in the scan head. If nuclear staining is not required, as for most applications relevant for LD research, this is a reasonable well-optimized imaging setup. The far-red channel, now occupied with an Alexa 647 dye, may also be used with a red fluorescent protein. In this case, it may be appropriate to use a 594-nm laser line instead of the 633-nm line.

Four-color imaging at the Zeiss LSM510

DAPI: 405-nm laser from a 25 mW diode laser at 3% laser power → HFT405/514/633 → sample → HFT405/514/633 → NFT635vis → mirror → BP420-480 → detector 2

EGFP: 458-nm line from a 30 mW Argon ion multi laser line at 25% laser power → HFT458/514 → sample → HFT458/514 → NFT635vis → NFT515 → BP505-550 → detector 2

LD540: 514-nm line from a 30 mW Argon ion multi laser line at 6% laser power → HFT458/514 → sample → HFT458/514 → NFT635vis → NFT515 → BP530-580 → detector 3

Alexa647: 633-nm line from a 5 mW HeNe laser at 5% laser power → HFT405/514/633 → sample → HFT405/514/633 → mirror → NFT515 → LP650 → detector 3

Comment: This implementation is on a different instrument, because our LSM510 META is not equipped with a 405-nm laser line for a DNA dye. The instrument used, in contrast, does not feature a 543-nm laser, which forced us to excite LD540 off-center with the 514-nm laser line. This is compensated by the dyes brightness and by the use of a BP530-580 that collects most of the emitted light. The 514-nm laser line also weakly excites EGFP, whose fluorescence is partially collected with the BP530-580, potentially causing bleed-through into the LD540 image. Practically, this was not observed, probably because the dye is much brighter than EGFP. A more severe problem was encountered in the EGFP channel. The instrument is optimized for EGFP excitation with a 488-nm laser line and does not offer the BP475-520 but a BP505-550 emission filter. Combined with the NFT515 to remove possible fluorescence from LD540, this results in a narrow band 505–515 nm collection of EGFP emission. This was partially compensated by increasing the excitation energy (25% versus 14% before). Image quality was sufficient for well-expressed EGFP constructs, but low-expressing constructs or those with a diffuse intracellular distribution may result in noisy images. Although this instrument is by far not optimal for our use, we obtained four-color images of a quality sufficient for many practical uses.

For live cell imaging on the Zeiss LSM510 META, dishes were placed in a temperature controlled aluminum block. The objective was a Zeiss Plan-APOCHROMAT 63x/NA1.0 VIS/IR water immersion lens directly dipping into the cell culture dish, heated to 37°C.

Acknowledgments

We thank Peter Pitrone (MPI-CBG) for making the Zeiss water immersion lens available. Financial support by the German National Academic Foundation (to J. S.) and the EC (FP7 LipidomicNet to C. T.) is gratefully acknowledged. Competing financial interests: The Max-Planck-Society has submitted a patent application on the use of LD540 for multicolor imaging.

Supporting Information

Additional Supporting Information may be found in the online version of this article:

Table S1: Lipophilicity of LD540 and Bodipy 493/503. Dyes were dissolved in octanol-saturated water or oil-saturated methanol at a concentration of 0.1 μg/mL, measured in the fluorometer and shaken with an equal volume of water-saturated octanol or methanol-saturated oil for 20 min. Phases were separated by centrifugation. For octanol/water coefficients, the concentration of dye in the water phase was measured and used for calculations of log *P*, which is defined as the decadic logarithm of the ratio of the substance's concentrations in the hydrophobic and the hydrophilic phase. For the oil/methanol system, 10 μL samples of both phases were taken, diluted into 990 μL of isopropanol and measured in the fluorometer. The ratio was used for calculation of log *P*. Values obtained in the octanol/water system indicated higher lipophilicity of LD540. Because log *P* values larger than 3 obtained by direct solvent partitioning are prone to errors, we also conducted measurements in the immiscible pair sunflower oil/methanol, where log *P* values for lipophilic substances are much smaller and less error prone. Note that in both solvent pairs LD540 has significantly larger values of log *P*, indicating higher lipophilicity. All values are average ± SD, p values were determined by Students *t*-test.

Table S2: Spectra in water, ethanol, hexane and sunflower oil were measured at 3×10^{-7}M. Differentiated 3T3-L1 cells were stained on the culture dish with 0.2 μg/mL (6.4×10^{-7}M) LD540 in DMEM +10% FCS for 30 min, followed by three washes. Cells were trypsinized and suspended in PBS at 100 000 cells/mL. All measurements were performed in quartz cuvettes on a Jobin Yvon Fluoromax3 spectrofluorometer. #Note that the excitation maximum fits to the one reported in the patent by Morgan and Boyer (Morgan LR, Boyer JH; Boron difluoride compounds useful in photodynamic therapy and production of laser light. USA patent 5,446,157. 1995), whereas the emission maximum in this patent was 560 nm. At the concentration used in the patent, that is, 2×10^{-4}M, we found a maximum of 557 nm (in a 4-mm cuvette), which decreased to 550 nm if a 1-mm cuvette was used, indicating that this redshift is due to inner filtering (Divya O, Mishra AK. Understanding the concept of concentration-dependent redshift in synchronous fluorescence spectra: prediction of lambda (SFS) (max) and optimization of Deltalambda for synchronous fluorescence scan. Anal Chim Acta 2008;630:47–56) at high concentration.

Table S3: Normalized excitation and emission spectra of LD540, Bodipy 493/503 and Nile Red, all measured at $3 \times 10 - 7$ M in sunflower oil. This excel file contains both the numerical values as well as graphic representations of the spectra.

Figure S1: Spectra of LD540 and other dyes used for multicolor imaging. A) Dyes were dissolved at 0.1 μg/mL in sunflower oil and excitation and emission spectra measured in a Yobin-Yvon Fluoromax 3 spectrofluorometer. Note the narrow emission peak of LD540, which is the basis of its use for multicolor imaging. B) Overlay of the LD540 spectra from Figure S1A with the fluorescence spectra of EGFP (from the Boswell and McNamara spectra collection at http://home.earthlink.net/~gfpology/McNamara_Boswell_Spectra_Dyes_FPs.zip). Position of laser lines and filter sets are indicated at the top of the picture. The broad excitation spectrum of EGFP allows excitation at 458 nm (61% efficiency), where LD540 is only weakly activated (5% eff.). A BP475-515-nm emission filter collects a large part of EGFP fluorescence (45% of total emission) but a negligible amount of the LD540 emission. Likewise, excitation of LD540 at 543 (93% eff.) or 532 nm (68% eff.) together with a LP560 nm filter collects enough light (37% of total emission) for bright images. C) Four-color imaging using LD540. Alongside with the spectra of the dyes used, the emission filter sets that were used for images in Figure 2B are indicated at the top of the figure. Note the large gap between the emission of LD540 and Alexa647, which might be filled with another dye with excitation by the 594-nm laser line and narrow band emission around 610 nm, for example, Texas Red.

Figure S2: Photostability of LD540. A) Dyes were dissolved at 0.1 μg/mL in sunflower oil (which represents the cellular environment of the dyes) and constantly irradiated in a photometer cuvette at their respective absorption maximum. Excitation energy was equal for all three dyes. Every 15 seconds, fluorescence emission was recorded. The plot shows a logarithmic representation of the normalized fluorescence values. The

slope of the curves are directly proportional to the respective rate of photobleaching. Under these conditions, LD540 is three times more stable than Nile Red and 15 times more stable than Bodipy 493/503. B) A431 cells were stained with Bodipy 493/503 (0.5 μg/mL) or LD540 (0.1 μg/mL) as described above. On a Zeiss LSM510 Meta, dyes were excited with a 488-nm or a 543-nm laser line, respectively, and imaging parameters were set for each dye individually to obtain optimal images. Repeated image frames were taken. On each series of frames, five regions of interest (ROIs), each containing several LDs, were defined. The pixel intensity values for each ROI were averaged to give the intensity that is plotted against the frame number. The resulting curve represents the bleaching rate that an experimentalist will encounter. Under these conditions, LD540 is about four times more stable than Bodipy 493/503, which corroborates the trend seen in Figure S2A.

Movie S1: COS7 cells transiently expressing tubulin-EGFP (green) were stained with LD540 (magenta) and images taken on the Zeiss LSM510 META every 4 seconds for a total of 120 seconds. The movie shows a section of 37 μm × 37 μm with a pixel size of 0.15 μm. The microtubules extend from the nucleus, which was at the upper left of the image, to the periphery of this cell.

Please note: Wiley-Blackwell are not responsible for the content or functionality of any supporting materials supplied by the authors. Any queries (other than missing material) should be directed to the corresponding author for the article.

References

1. Wolins NE, Quaynor BK, Skinner JR, Schoenfish MJ, Tzekov A, Bickel PE. S3-12, Adipophilin, and TIP47 package lipid in adipocytes. J Biol Chem 2005;280:19146–19155.
2. Greenspan P, Mayer EP, Fowler SD. Nile red: a selective fluorescent stain for intracellular lipid droplets. J Cell Biol 1985;100:965–973.
3. Gocze PM, Freeman DA. Factors underlying the variability of lipid droplet fluorescence in MA-10 Leydig tumor cells. Cytometry 1994;17:151–158.
4. Miura S, Gan JW, Brzostowski J, Parisi MJ, Schultz CJ, Londos C, Oliver B, Kimmel AR. Functional conservation for lipid storage droplet association among Perilipin, ADRP, and TIP47 (PAT)-related proteins in mammals, drosophila, and dictyostelium. J Biol Chem 2002;277:32253–32257.
5. Granneman JG, Moore HP, Mottillo EP, Zhu Z. Functional interactions between Mldp (LSDP5) and Abhd5 in the control of intracellular lipid accumulation. J Biol Chem 2009;284:3049–3057.
6. Invitrogen. HCS LipidTOX™ neutral lipid stains. 2006. Available from: http://www.probes.invitrogen.com/media/pis/mp34475.pdf Accessed date 9/3/09.
7. Loudet A, Burgess K. BODIPY dyes and their derivatives: syntheses and spectroscopic properties. Chem Rev 2007;107:4891–4932.
8. Morgan LR, Boyer JH, inventors. Boron difluoride compounds useful in photodynamic therapy and production of laser light. USA Patent 5,446,157. 1995.
9. Listenberger LL, Brown DA. Fluorescent detection of lipid droplets and associated proteins. Curr Protoc Cell Biol 2007;Chapter 24: Unit 24.2.
10. Stemmer A, Beck M, Fiolka R. Widefield fluorescence microscopy with extended resolution. Histochem Cell Biol 2008;130: 807–817.
11. Pol A, Martin S, Fernandez MA, Ferguson C, Carozzi A, Luetterforst R, Enrich C, Parton RG. Dynamic and regulated association of caveolin with lipid bodies: modulation of lipid body motility and function by a dominant negative mutant. Mol Biol Cell 2004;15: 99–110.
12. Turro S, Ingelmo-Torres M, Estanyol JM, Tebar F, Fernandez MA, Albor CV, Gaus K, Grewal T, Enrich C, Pol A. Identification and characterization of associated with lipid droplet protein 1: a novel membrane-associated protein that resides on hepatic lipid droplets. Traffic 2006;7:1254–1269.
13. Welte MA, Cermelli S, Griner J, Viera A, Guo Y, Kim DH, Gindhart JG, Gross SP. Regulation of lipid-droplet transport by the perilipin homolog LSD2. Curr Biol 2005;15:1266–1275.
14. Shubeita GT, Tran SL, Xu J, Vershinin M, Cermelli S, Cotton SL, Welte MA, Gross SP. Consequences of motor copy number on the intracellular transport of kinesin-1-driven lipid droplets. Cell 2008;135:1098–1107.
15. Bostrom P, Rutberg M, Ericsson J, Holmdahl P, Andersson L, Frohman MA, Boren J, Olofsson SO. Cytosolic lipid droplets increase in size by microtubule-dependent complex formation. Arterioscler Thromb Vasc Biol 2005;25:1945–1951.
16. Boulant S, Douglas MW, Moody L, Budkowska A, Targett-Adams P, McLauchlan J. Hepatitis C virus core protein induces lipid droplet redistribution in a microtubule- and dynein-dependent manner. Traffic 2008;9:1268–1282.
17. Roohvand F, Maillard P, Lavergne JP, Boulant S, Walic M, Andreo U, Goueslain L, Helle F, McLauchlan J, Budkowska A. Initiation of hepatitis C virus infection requires the dynamic microtubule network: role of the viral nucleocapsid protein. J Biol Chem 2009;284:13778–13791.
18. Hirokawa N, Takemura R. Kinesin superfamily proteins and their various functions and dynamics. Exp Cell Res 2004;301:50–59.
19. Kuerschner L, Moessinger C, Thiele C. Imaging of lipid biosynthesis: how a neutral lipid enters lipid droplets. Traffic 2008;9:338–352.
20. Fukumoto S, Fujimoto T. Deformation of lipid droplets in fixed samples. Histochem Cell Biol 2002;118:423–428.